Transitions to spatiotemporal chaos and turbulence of flute instabilities in a low-β magnetized plasma

F. Brochard,* E. Gravier, and G. Bonhomme
LPMIA, UMR 7040 du CNRS, Université Henri Poincaré, Boîte Postale 239, F-54506 Vandoeuvre-les-Nancy Cedex, France
(Received 2 December 2005; published 6 March 2006)

The spatiotemporal transition scenario of flute instabilities from a regular to a turbulent state is experimentally investigated in the low-β plasma column of a thermionic discharge. The same transition scenario, i.e., the Ruelle-Takens route to turbulence, is found for both the Kelvin-Helmholtz and the Rayleigh-Taylor instabilities. It is demonstrated that the transition can be more or less smooth, according to the discharge mode. In both cases, a strong radial dependence is observed, which is linked to the velocity shear layer in the case of the Kelvin-Helmholtz instability.

DOI: 10.1103/PhysRevE.73.036403 PACS number(s): 52.35.Ra, 05.45.−a, 52.35.Py

I. INTRODUCTION

The Kelvin-Helmholtz and Rayleigh-Taylor instabilities are of concern in a variety of phenomena which occur in fluid dynamics, space, and astrophysical plasmas, fusion and laboratory plasmas where they are also called flute instabilities [1]. Their linear stability in incompressible hydrodynamic and magnetohydrodynamic fluids is well known for several decades [2]. Since then, several studies have extended the description to the compressible case. However, to our knowledge, the experimental observation of their transition to turbulence has never been reported. We demonstrated very recently our ability to produce and select these instabilities in a magnetized plasma [3]. Laboratory plasmas, due to a variety of control parameters, are well suited to investigate nonlinear phenomena, and have attracted much attention from the nonlinear dynamics community. First observations of period doubling and intermittent routes to chaos in plasmas were reported in the late 1980s [4,5]. Since then, spatially extended plasmas have been shown to exhibit rich dynamical behaviors, leading to pattern formation, spatiotemporal chaos, or turbulence [6–8], which is a common feature of spatially extended dissipative systems [9]. In this paper, we present the experimental observation of the transition of flute instabilities from a regular state to spatiotemporal chaos.

This paper is organized as follows. In Sec. II we present the plasma device and we justify our choice of the discharge voltage U_d as a control parameter. In Sec. III we consider the case of a Kelvin-Helmholtz instability. Two transitions to turbulence are described, a smooth one, which occurs when U_d is increased, and a brutal one which occurs when U_d is decreased at relatively low discharge voltages. Though the transition scenario of a Rayleigh-Taylor instability is basically the same as for the Kelvin-Helmholtz instability, some differences exist, which are presented in Sec. IV. Last, main results are summarized in Sec. V.

II. EXPERIMENTAL SETUP

The study is performed in the central chamber of the triple plasma device MIRABELLE [10] (Fig. 1), operated in argon gas. A limiter, 15 cm in diameter, is inserted between the source chamber and the central chamber in order to enhance the radial equilibrium electric field, and thus the plasma rotation, which is a necessary condition to produce a flute instability in such a device. Main parameters of the plasma are listed in Table I, and the setup for the selection of flute instabilities is detailed in Ref. [3]. Temporal analysis is based on time series of the floating potential measured at various radial positions. Though plasma potential and floating potential profiles are very different in this device due to primary ionizing electrons on the axis of the column, electron temperature fluctuations can be ignored, and thus we can make the assumption that plasma potential and floating potential fluctuations are in phase [3]. Spatiotemporal data are directly obtained from a circular array of 32 probes, which records the density fluctuations at the fixed radius $r=7$ cm.

At first sight, this diagnostic could present two weak points: in a general way it is more perturbative than other diagnostic tools, such as the use of a two-tips probe to estimate the azimuthal wave number of a propagating mode [11], and the fixed radial location does not allow to perform measurements at the maximum of amplitude of the modes, located at a lower radius, between 3 and 5 cm. However, a

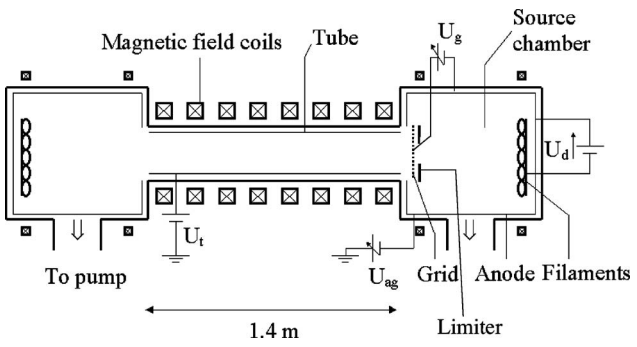

FIG. 1. The MIRABELLE plasma device (the limiter is connected to the anode).

*Electronic address: frederic.brochard@lpmi.uhp-nancy.fr

TABLE I. Main plasma parameters in MIRABELLE.

Operating pressure (Argon)	2×10^{-4} mbar
Plasma density	$10^{15}-10^{16}$ m^{-3}
Electron temperature	1–4 eV
Ion temperature	$\leqslant$0.05 eV
Density gradient length	1–4 cm
ρ_s	0.2–1.5 cm
ω_{ci}	$0.5-3\times10^5$ rad s^{-1}
$\omega_{E\times B}$	$1.2-5\times10^4$ rad s^{-1}

positive effect of this location is that the array becomes much less perturbative to the plasma: the signal recorded with a movable probe inside the plasma column does not exhibit any change neither in phase nor in amplitude whatever the usual bias applied to the external array. Moreover, it offers a very good spatiotemporal resolution over a complete circumference of the plasma column, which is needed to ensure that the transition to turbulence is of a spatiotemporal nature. Last, to complete the apparatus, two field-aligned Langmuir probes distant of 40 cm are used to check that the parallel wave number remains negligible during the transition, which ensures we are still dealing with flute modes.

The transition from a regular state to turbulence is obtained by varying a control parameter which has to be carefully chosen. Flute instabilities, triggered by the plasma rotation, are sensitive to any variation of the radial equilibrium electric field. The latter can be varied by adjusting the biasing of a separation grid located between the source chamber and the central chamber [12], making this bias a possible control parameter. However, varying the discharge voltage U_d is found to be more efficient by acting directly on the discharge current, which allows us to study the transition to turbulence in different discharge modes [13,14]. Though the transitions described in this paper are both observed in the temperature limited mode (TLM) [13], in which the discharge current is limited only by the cathode temperature, it is useful to introduce a distinction between a high-TLM in which a first, smooth transition to turbulence is observed when increasing the discharge voltage, and a low-TLM, in which a brutal transition occurs when U_d is decreased. Here, the term *high* stands for values of U_d higher than $\sim$25 V, whereas *low* stands for values of U_d in the range 20–25 V. Decreasing U_d from 70 V to 20 V also leads to a reduction of the mean density in the central part of the column (minus 10–50 % according to the other discharge parameters). By visual inspection of the plasma column, one can notice the transition from a luminous beam of plasma in the high-TLM (when a diaphragm is present) to a pale and diffused halo in the low-TLM. Decreasing U_d lower than 20 V then leads to a transition to another discharge mode, called Langmuir mode (LM) [13,14], in which the space charge in the cathode region is not fully neutralized by the weak ion flux. Although we approach this transition, we do not study LM oscillations in this paper.

III. TRANSITION TO TURBULENCE OF A KELVIN-HELMHOLTZ INSTABILITY

A. Transition in the high-TLM

It is found that two transitions can occur according to the equilibrium discharge mode. The first scenario is observed when increasing U_d in the high-TLM. Increasing U_d and keeping all the other discharge parameters unchanged, one obtained for a Kelvin-Helmholtz instability the bifurcation diagram depicted in Fig. 2. The bifurcation sequence can be divided into four major areas *A*-*B*-*C*-*D*, separated by dashed lines in the figure. At lower values of U_d, a regular mode is seen, characterized by a narrow peak at a frequency f_1 $\sim$7–7.5 kHz (*A* area). From spatiotemporal analysis [Figs. 3(a)–3(c)] it is found that this state corresponds to a well established $m=1$ mode. When U_d is increased upon 44 V, the bifurcation diagram broadens consecutively to the onset of a new peak close to the first harmonics of the $m=1$ mode (*B* area). Time series are much less regular and temporal analysis with a wavelet transform shows aperiodic losses of synchronization, with vertical sidebands corresponding to the widening of the frequency spectrum [Figs. 3(d) and 3(e)]. Bifurcations between $m=1$ and $m=2$ are observed in the spa-

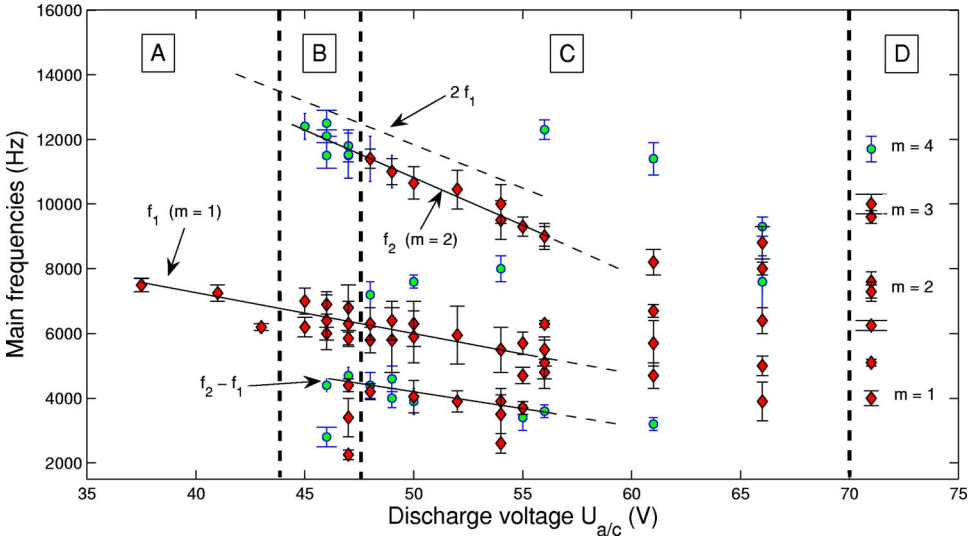

FIG. 2. (Color online) Bifurcation diagram of a Kelvin-Helmholtz instability in the high-TLM, from time series recorded at $r=5$ cm. Main peaks are indicated with diamonds, and circles designate peaks of lower intensity. The error bars represent the half-magnitude width of the peaks. Lines are drawn to guide the eye.

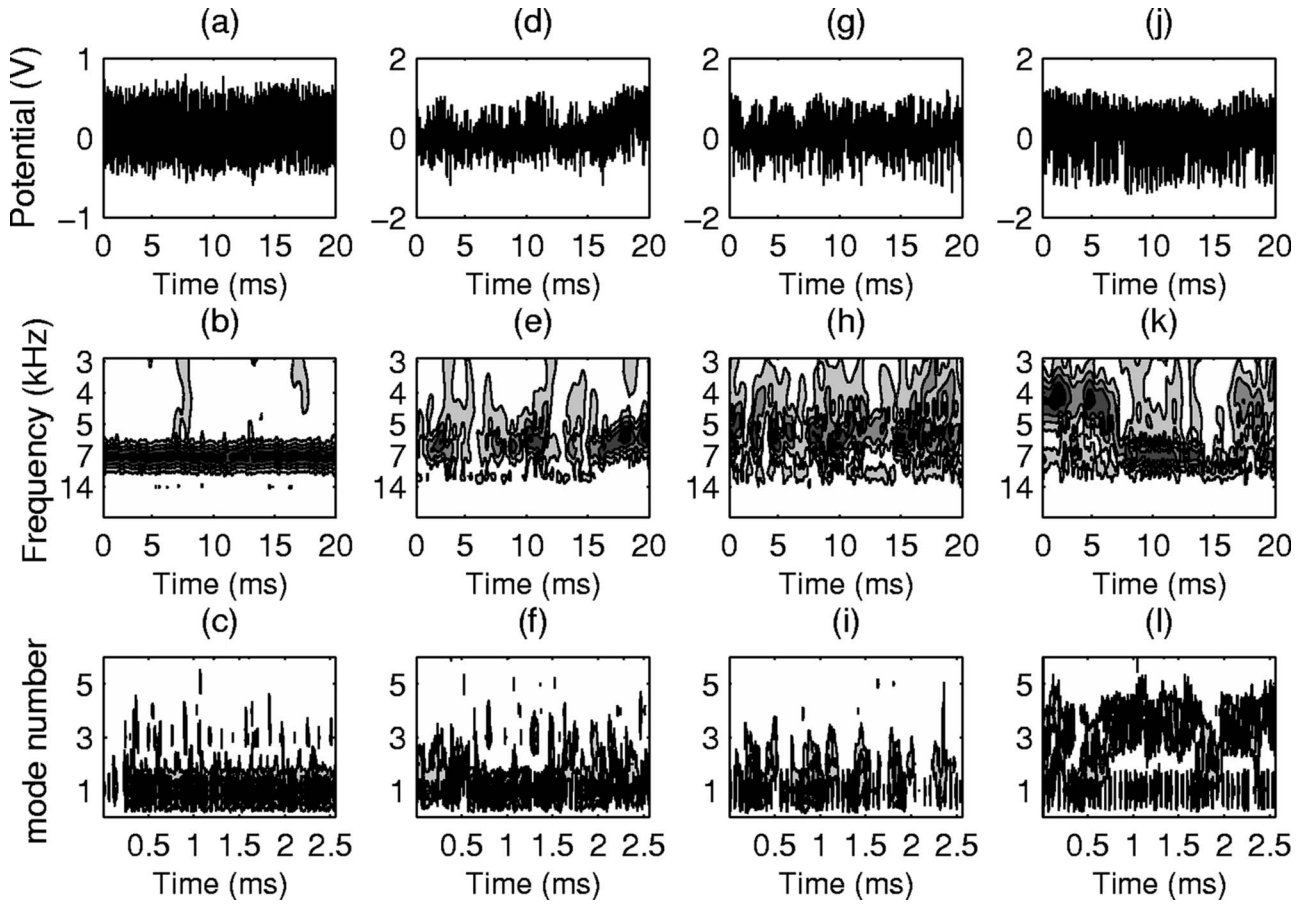

FIG. 3. Transition to turbulence of a Kelvin-Helmholtz instability in the high-TLM: time series recorded at $r=5$ cm, wavelet transform, and spatial Fourier transform showing the evolution of the mode number over the time at $r=7$ cm, for each regime depicted in Fig. 2. The control parameter values are (a)–(c) $U_d=37$ V, (d)–(f) $U_d=46$ V, (g)–(i) $U_d=50$ V, (j)–(l) $U_d=71$ V.

tiotemporal image (not figured here) as well as in the spatial Fourier transform of the signal recorded on the azimuthal array of probes [Fig. 3(f)]. Reconstructions of the phase portrait of the whole time series do not exhibit particular structure, whereas reconstructions limited to regular samples of the time series exhibit a two torus, which is the signature of a quasiperiodic state interspersed with chaotic bursts. Because of the nonlinearity of the dispersion relation, nonlinear interactions between the $m=2$ mode at the frequency $f_2 \sim 10.5$ kHz, and the $m=1$ mode at $f_1 \sim 6$ kHz and its first harmonics produce new frequencies which broaden the spectrum. When U_d is further increased, peaks are less pronounced and wider, which results in larger error bars in Fig. 2 (C area). The frequency power spectrum becomes more and more broad, noiselike, as U_d is increased, making more and more complicated to plot the bifurcation diagram. Temporal and spatiotemporal analysis show strongly irregular behavior corresponding to a chaotic state [Figs. 3(g)–3(i)].

Although we do not have definite proof, it is expected that the strengthening of the nonlinear interactions leading to turbulence is due to the tightening of the plasma column while U_d is increased. Increasing the discharge current leads to fluctuations localized closer to the axis of the plasma column, as it can be easily observed when a regular state is considered. Thus, when several modes coexist, it is expected that increasing U_d moves the maximum of amplitude of each mode closer, reinforcing the nonlinear interactions between them. Partly because of this radial evolution in the location of the maximum of amplitude of the m mode, a radial dependance has also to be taken into account in the characterization of the transition to turbulence. In the case of the Kelvin-Helmholtz instability, this characteristic is strengthened by the limited radial extension of the velocity shear layer. With the chosen set of parameters, the maximum of this layer is located between $r=3$ and $r=5$ cm.

Thus, Figs. 2 and 3 give information only about the fluctuations located outside or in the outer part of the velocity shear layer. Analyzing signals recorded inside the latter can give crucial information to understand the complex dynamics of this instability. Figure 4 represents a time series recorded in the middle of the shear layer and the time evolution of its frequency, at $U_d=50$ V. This signal is characterized by a periodic modulation, both in amplitude and in phase, which makes it very different from the signal recorded in the same experimental conditions at $r=5$ cm [Figs. 3(g) and 3(h)]. It corresponds to a particular quasiperiodic state known as periodic pulling [15]. In that case, we observe an incomplete synchronization of $m=1$ by $m=2$, the latter acting as the excitator of an oscillator. Here the amplitude and/or the frequency mismatch between both modes is too large to ensure

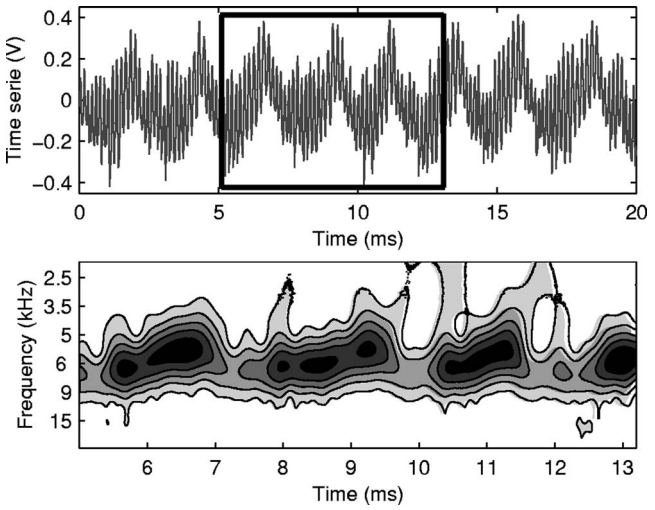

FIG. 4. Time series recorded in the shear layer at $r=4$ cm, and detail of the wavelet transform, showing periodic sliding of the frequency ($U_d=50$ V).

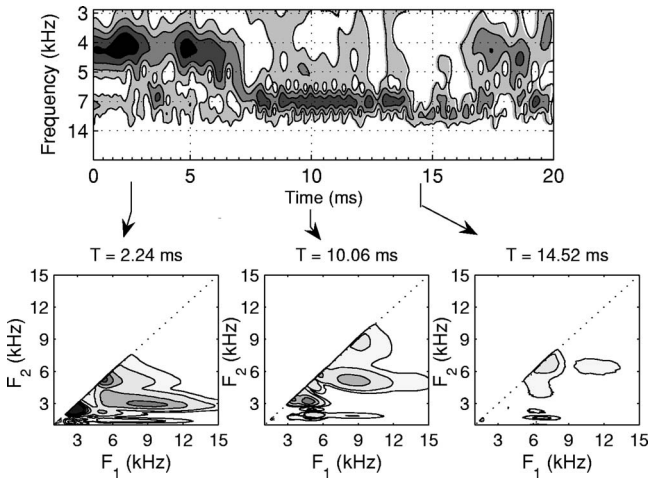

FIG. 5. Analysis of the intermittent state recorded in the *D* part of Fig. 2. The upper graph is a zoom of Fig. 3(k) showing the time evolution of the frequency. Below is plotted the wavelet bicoherence at three representative times. The large horizontal structure in the plot at time 2.24 ms indicates phase coupling between the frequency 3 kHz and frequencies in the range 6–15 kHz. Another horizontal structure can be distinguished in the bottom part of the plot, which reveals phase coupling between the frequency 2 kHz and frequencies 3–11 kHz. At time 10.06 ms, these structures are shifted, and the main coupling is observed between 5 kHz and frequencies 7–12 kHz. On the contrary, coupling at time 14.52 ms is very weak, of the same order of magnitude as the statistical noise due to the wavelet decomposition [18]. Contours are shown at values 0.02, 0.05, 0.15, 0.25, 0.35, and 0.45.

complete synchronization, but it is sufficiently small to reach synchronization periodically. Such a behavior can be easily reproduced with simple temporal models, e.g., considering a Van der Pol oscillator [16,17]. In our experiments, periodic pulling has been observed only inside the velocity shear layer, probably because it is the only place where the fragile equilibrium needed between both modes is satisfied, $m=1$ dominating in the central part of the column while larger mode numbers dominate in its outer part. More generally, it is remarkable that quasiperiodicity is more pronounced in the shear layer than in the external layers of the plasma, where the behavior is more chaotic or randomlike.

At this point, the chain of events is essentially the same as the one already observed with drift waves, and known as the quasiperiodicity or Ruelle-Takens route to turbulence [6]. However, when the control parameter reaches a critical value, a new phenomenon is observed. At $U_d=70$ V, the bifurcation diagram cannot be plotted because the frequency power spectrum is too broad, but at $U_d=71$ V the power spectrum exhibits several narrow frequency peaks. Purely temporal analysis shows separate time windows where synchronization to a main frequency is achieved [Figs. 3(j) and 3(k)]. Spatiotemporal analysis shows evidences that these frequencies correspond to various mode numbers, $m=1$, 2, 3, and 4 being alternately observed [Fig. 3(l)]. Although there are more different modes than previously, the narrowness of the frequency power spectrum peaks seems to indicate that few interactions occur between them. Nevertheless, a more careful analysis based on the use of the wavelet bicoherence [18] demonstrates that nonlinear coupling between a reduced number of modes still exists. Bicoherence at three selected times is plotted in the lower part of Fig. 5. Only the low-frequency range is represented, since almost no coupling is seen at higher values. This figure shows that the coupled frequencies differs in each time window of the recorded signal. Phase coupling is significant only in the two first windows considered, dominated respectively by the frequencies 4 kHz and 7 kHz, and almost negligible in the third time window dominated by the frequency 12 kHz. Thus, it results that this state is characterized by an alternation between two distinct quasiperiodic states and an almost regular state. For the same discharge voltage $U_d=71$ V, the analysis of a signal recorded in the middle of the shear layer confirms the alternation between different modes. Nevertheless, lower frequency modes, $m=1$ and $m=2$, are favored by the drop in the rotation velocity. As a consequence, $m=3$ and especially $m=4$ seem to be missing, which results in a more quasiperiodic signal. Unfortunately, a further increase of U_d leads to electric arcs in the plasma column, making it impossible to investigate the evolution of this state beyond $U_d=75$ V.

B. Transition approaching the Langmuir mode in the low-TLM

A second transition can also be observed when decreasing U_d when approaching the transition from TLM to Langmuir mode [13]. In that case, fluctuations are very sensitive to any change of the control parameter, since a drop of only 2 V in U_d causes the transition from a regular $m=1$ mode [Fig. 6(a)] to turbulence [Fig. 6(c)], via a quasiperiodic state [Fig. 6(b)]. Here again periodic pulling between $m=1$ and $m=2$ is observed but only in a very narrow range of the control parameter, producing the characteristic modulation of the signal already seen in Fig. 4, and giving to the power spectrum an easily recognizable asymmetric shape [Fig. 6(b)]. In contrast to what is observed in the high-TLM, the plasma diameter is bigger and fluctuations are much less localized. Strict quasi-

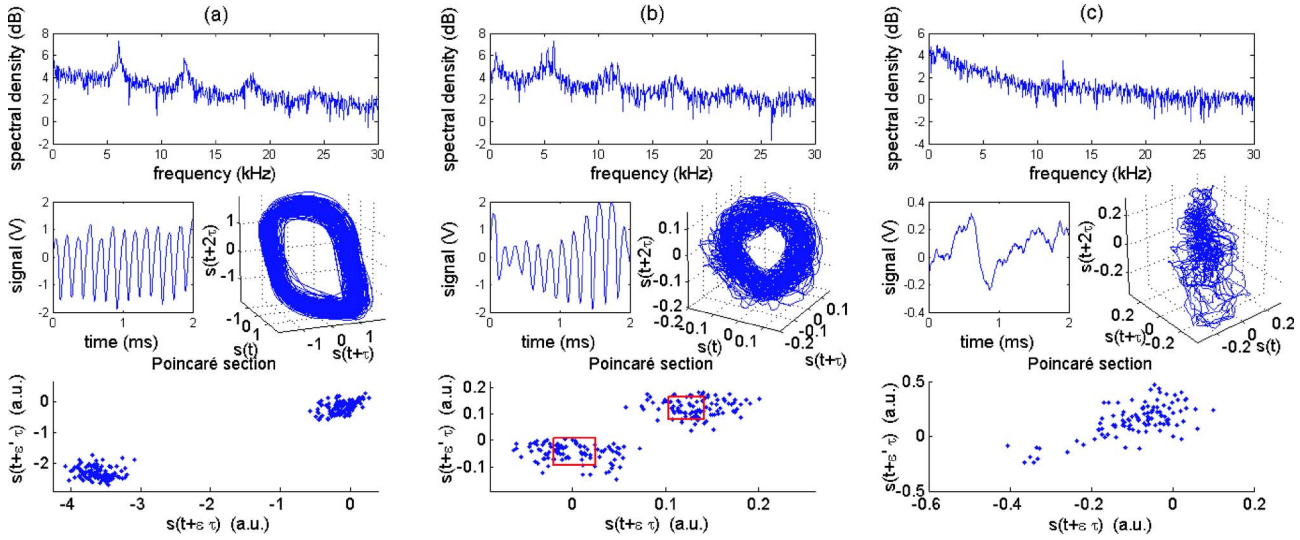

FIG. 6. (Color online) Fast transition to turbulence of a flute instability: frequency power spectrum, detail of the time series recorded at $r=4$ cm, phase space embedded in $d=3$ dimension, and Poincaré section of the regular state (a), quasi-periodic state (b), and turbulent state (c). $S(t+\tau)$ is the time series at the time $t+\tau$, where τ is the delay time, which corresponds to the first zero of the autocorrelation function. The Poincaré sections are computed at given angles, related to the parameters ϵ and ϵ' (axes are not the same as in the phase portrait). The control parameter values are (a) $U_d=23.5$ V, (b) $U_d=22.5$ V, (c) $U_d=21.5$ V.

periodicity is recorded in a quite large radial extent of the plasma column, between $r=3$ and $r=6$ cm, which corresponds approximately to the location of the velocity shear layer. Thus it is expected that the maximum of amplitude of each mode is not as localized as in the high-TLM. It results that nonlinear coupling between the various modes should exist in a larger radial extent of the plasma column, which could explain the fastest transition to turbulence.

IV. TRANSITION TO TURBULENCE OF A RAYLEIGH-TAYLOR INSTABILITY

When a Rayleigh-Taylor instability is selected [3], the same transition scenario, i.e., the quasiperiodicity route is observed, with slight differences. In particular, the D part of the bifurcation diagram is never seen, although the transition can be observed both in the low- and high-TLM. The other differences, that we now discuss in more detail, indicate that Rayleigh-Taylor modes do not present the same spatiotemporal features (i.e., structure, dispersion relation) than the Kelvin-Helmholtz or the drift wave ones.

First, it is noticeable that nonlinear interactions are stronger in the medium part of the plasma than in its outer part: starting from a regular state, every step on the way to turbulence is first observed at $r=3$ cm, and then at $r=6$ cm. For example, simultaneous recordings at both locations show that quasiperiodicity first appears at $r=3$ cm, time series being at the same moment 1 periodic at $r=6$ cm. When U_d is varied, quasiperiodicity is then observed at both locations: contrary to the Kelvin-Helmholtz instability, quasiperiodicity, including periodic pulling, can be observed in a large radial extent of the column, in the high-TLM as well as in the low-TLM. Considering Fig. 7, which represents time series recorded simultaneously at both locations in a periodic pulling state, one can notice that there are more beats at $r=3$ cm than at $r=6$ cm. In linear models, the beat frequency of two waves is the difference between the frequencies f_1 and f_2 of the respective waves. Although modes considered

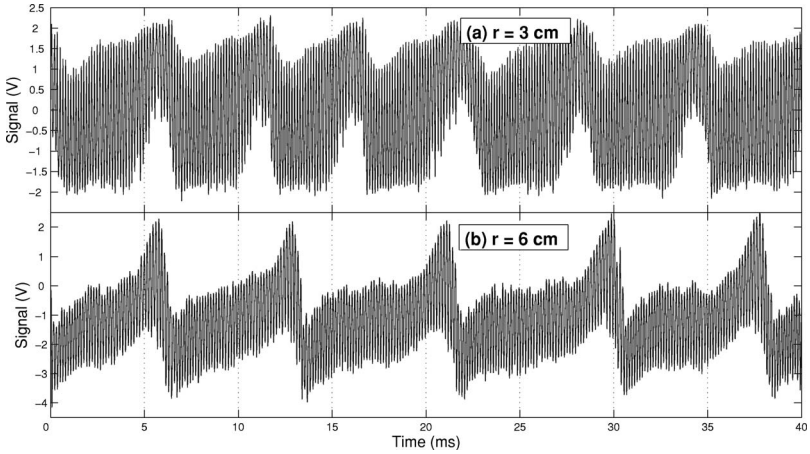

FIG. 7. Time series of the floating potential recorded simultaneously at $r=3$ cm (a), and at $r=6$ cm (b), for a Rayleigh-Taylor instability in a quasi-periodic state. The beat frequency is lower at $r=6$ cm.

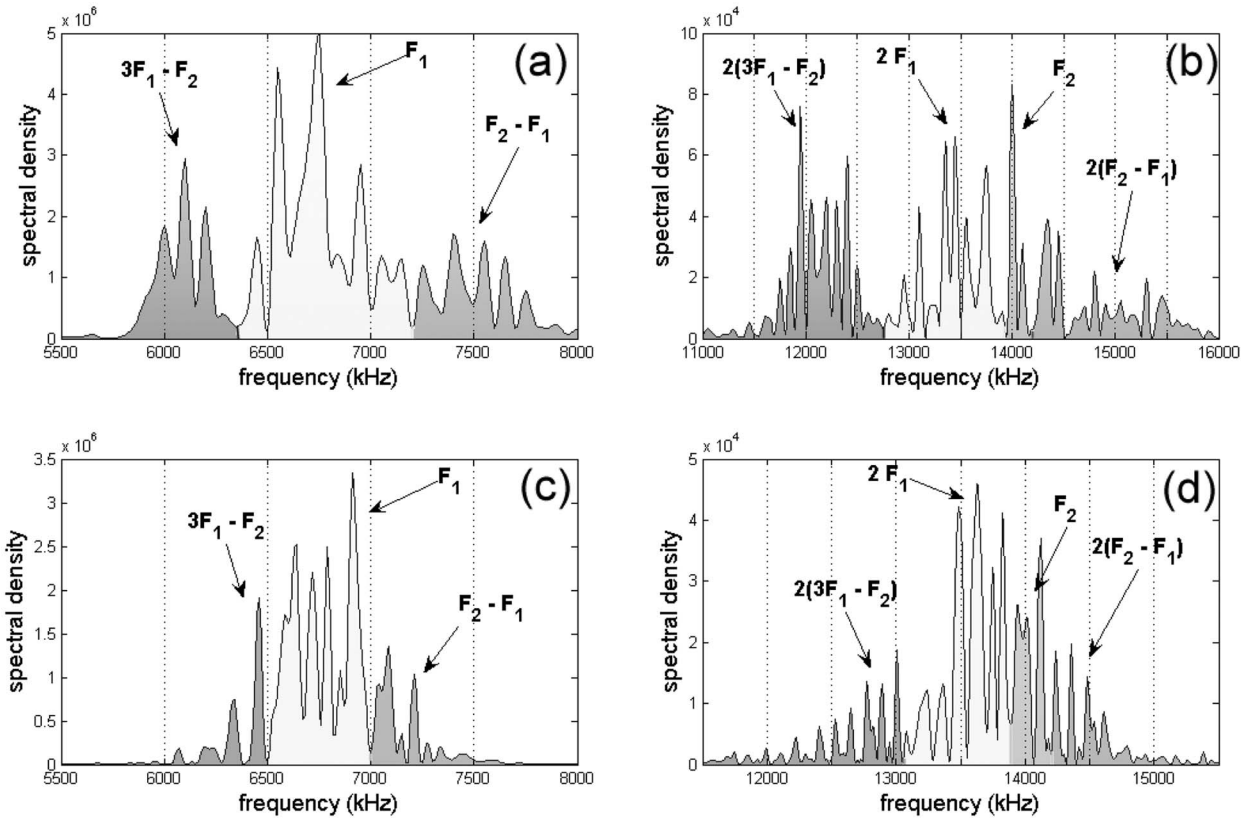

FIG. 8. Fourier spectrum of the quasi-periodic signals shown in Fig. 7: main frequencies (left) and zoom on the first harmonics (right) of the signal recorded at $r=3$ cm (a,b), and at $r=6$ cm (c,d). F_1 and F_2 are respectively the frequencies of the $m=1$ and $m=2$ modes.

here interact nonlinearly, broadening the frequency spectrum, the same behavior is qualitatively observed, and we notice that the two interacting frequencies of the quasiperiodic state are always closer in the outer part of the plasma, where the beat frequency is lower, than in its inner part. This fact explains why the frequency spectrum is wider at $r=3$ cm than at $r=6$ cm (Fig. 8), and consequently why turbulence first arises at $r=3$ cm. Moreover, since each frequency of a quasiperiodic spectrum can be written as a linear combination of two frequencies, it is possible to estimate these frequencies from the location of the various peaks of the frequency spectrum. Whatever the time series, only one combination gives the location of each peak correctly (e.g., Fig. 8). From that result, we can conclude that contrary to drift waves and to the Kelvin-Helmholtz instabilities, the frequency f_2 of the $m=2$ mode of a Rayleigh-Taylor instability is more than twice the frequency f_1 of the $m=1$ mode. However, the gap between f_2 and $2f_1$ is rather small, of the order of 700 Hz at $r=3$ cm and 300 Hz at $r=6$ cm in the quasiperiodic state. Since it is a necessary condition to destabilize a Rayleigh-Taylor instability that the angular momentum does not increase with the radius [2], there is a constraint to the radial increase in the rotation frequency of the column, which probably explains the small gap between f_1 and f_2.

When U_d is further varied, this gap falls down and can even vanish, giving birth to a mode locking state in the outer part of the plasma when f_2 is exactly twice f_1 (Fig. 9). Although we did not observe this state with a Kelvin-Helmholtz instability, mode locking occurs during the transition to turbulence of drift waves as well [6], suggesting that it is a rather common phenomenon. However, recordings shows that strict mode locking exists only in a short range of variation of the control parameter, and in a narrow layer of the plasma, since simultaneous measurements at a lower radial location give evidence of a chaotic state (Fig. 10). Moreover, any slight variation of the control parameter in the mode-locking state leads to occasional losses of periodicity, which cause excursions outside the periodic double-loop or-

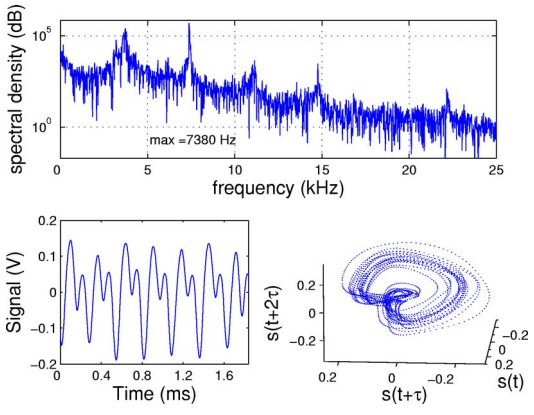

FIG. 9. (Color online) Fourier spectrum, detail of the time series of the floating potential, and phase portrait of the signal recorded at $r=5$ cm, for a Rayleigh-Taylor instability. In spite of some noise, the double loop phase space attractor is characteristic of a mode locking state.

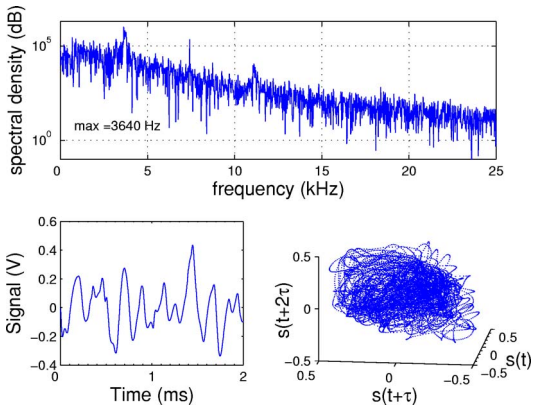

FIG. 10. (Color online) Fourier spectrum, detail of the time series of the floating potential, and phase portrait of the signal recorded at $r=3$ cm, for the same Rayleigh-Taylor state as the one depicted in Fig. 9: chaotic state.

bit in the phase portrait. This irregular behavior broadens the spectrum and leads to a chaotic state, and then to turbulence.

V. CONCLUSION

In conclusion, we have reported on experimental observations of the transition to turbulence of flute instabilities in a magnetized plasma. The Ruelle-Takens scenario, in which spatiotemporal chaos and turbulence result from nonlinear interactions between two modes with incommensurate frequencies, has been identified as a common route to turbulence for both the Kelvin-Helmholtz and the Rayleigh-Taylor instabilities, as it is for drift waves [6]. However, contrary to drift waves, spatiotemporal chaos is not necessarily associated with the onset of the $m=1$ mode. Moreover, it is pointed out that both the radial and the azimuthal dimensions have to be taken into account in the description of the transition. Particularly, in the case of the Kelvin-Helmholtz instability, it is found that quasiperiodicity is more clear inside the velocity shear layer, dynamics being more chaotic or intermittentlike in the external layers of the plasma. When a Rayleigh-Taylor instability is considered instead, the analysis of the quasiperiodic state suggests a different form of the dispersion relation, with a frequency growing faster than the m mode. However, experimental investigation of the dispersion relation and of the spatiotemporal structure of the azimuthal modes remains a very challenging task. For that reason, it would be of great interest to investigate the linear properties of the flute modes with an analysis based on the resolution of the eigenmode equation in a cylindrical geometry. Of great interest as well would be the confrontation of our results on the transition to turbulence with rigorous fluid simulations in the same geometry.

[1] G. I. Kent, N. C. Jen, and F. F. Chen, Phys. Fluids **12**, 2140 (1969).
[2] S. Chandrasekhar, *Hydrodynamic and Hydromagnetic Stability* (Oxford University Press, London, 1961), Chap. XI.
[3] F. Brochard, E. Gravier, and G. Bonhomme, Phys. Plasmas **12**, 062104 (2005).
[4] P. Y. Cheung and A. Y. Wong, Phys. Rev. Lett. **59**, 551 (1987).
[5] J. Qin, L. Wang, D. P. Yuan, P. Gao, and B. Z. Zhang, Phys. Rev. Lett. **63**, 163 (1989).
[6] T. Klinger, A. Latten, A. Piel, G. Bonhomme, T. Pierre, and T. Dudok de Wit, Phys. Rev. Lett. **79**, 3913 (1997).
[7] A. Atipo, G. Bonhomme, and T. Pierre, Eur. Phys. J. D **19**, 79 (2002).
[8] M. J. Burin, G. R. Tynan, G. Y. Antar, N. A. Crocker, and C. Holland, Phys. Plasmas **12**, 052320 (2005).
[9] M. C. Cross and P. C. Hehenberg, Rev. Mod. Phys. **65**, 851 (1993).
[10] T. Pierre, G. Leclert, and F. Braun, Rev. Sci. Instrum. **58**, 6 (1987).
[11] J. M. Beall, Y. C. Kim, and E. J. Powers, J. Appl. Phys. **53**, 3933 (1982).
[12] E. Marden Marshall, R. F. Ellis, and J. E. Walsh, Plasma Phys. Controlled Fusion **28**, 1461 (1986).
[13] K. G. Hernqvist and E. O. Jonhson, Phys. Rev. **98**, 1576 (1955).
[14] F. Greiner, T. Klinger, H. Klostermann, and A. Piel, Phys. Rev. Lett. **70**, 3071 (1993).
[15] M. E. Koepke, A. Dinklage, T. Klinger, and C. Wilke, Phys. Plasmas **8**, 1432 (2001).
[16] B. Van der Pol, Philos. Mag., Suppl. **73** (13), 65 (1927).
[17] F. Brochard, E. Gravier, G. Bonhomme, Proceedings of the 31st EPS Conference on Controlled Fusion and Plasma Physics, London, 2004 (unpublished).
[18] B. Ph. van Milligen, C. Hidalgo, and E. Sanchez, Phys. Rev. Lett. **74**, 395 (1995).